Tomographic Reconstruction of Band-limited Hermite Expansions

Wooram Park and **Gregory S. Chirikjian**
Department of Mechanical Engineering, Johns Hopkins University, Baltimore, MD, USA

Abstract

In this work, we investigate the parallel-beam projection and reconstruction of band-limited Hermite expansions. Using a recently developed coordinate conversion technique, we show how the Fourier slice theorem can be directly applied. In our new approach, we do not introduce a non-integrable filter that appears in the filtered backprojection method. Since a projection of a 2D band-limited Hermite expansion is a 1D band-limited Hermite expansion and the coordinate conversion technique is lossless with this special expansion, we can avoid a series of approximations that the classical tomography techniques make.

Keywords

Parallel-beam tomography; Hermite expansion; polar-Cartesian interpolation

1. INTRODUCTION

The Fourier slice theorem states that the Fourier transform of a projection of a 2D function is equal to the slice of the 2D Fourier transform of the function along a line through the origin in the frequency domain and tilted by the angle with which the projection is taken. While the 2D Fourier transform can be obtained by filling the frequency domain with the slices computed from projections, and its inverse Fourier transform gives the original 2D function, this direct scheme has not been adopted widely, since the slices form samples of the Fourier transform on a polar grid and samples on a Cartesian grid are needed for the inverse Fourier transform. This means that a polar-Cartesian coordinate conversion is required. This conversion can be thought of as interpolation between two sets of discrete samples in polar and Cartesian grids as shown in Fig. 1. Pan et al.[1] compared the local interpolation method and filtered backprojection method in a special type of tomography. Miao et al.[2] used pseudopolar Fourier transform and oversampling technique to handle this coordinate conversion problem. However on an equally spaced polar grid, samples can be sparse for large values of radius, which leads to poor resolution of high frequency features when the interpolation is performed in the frequency domain. This leads to degradation of the details of the image.

In order to avoid this interpolation problem, the filtered backprojection algorithm is widely used. The filtered backprojection algorithm can be derived from the Fourier slice theorem. A filter in the frequency domain naturally appears in the formulation. However, since the filter is not square-integrable, its inverse Fourier transform should be approximated in some way. This is also an inexact step. In our work, we assume that the original 2D function can be described as a band-limited Hermite expansion, and we apply the Fourier slice theorem directly to solve the tomography problem. We investigate the relative benefit of this special band-limited expansion as compared to the classical filtered backprojection method.

2. METHOD

2.1. Hermite Expansions and Related Preliminary Work

Hermite polynomials are solutions to the differential equation

$$y'' - 2xy' + 2ny = 0,$$

and are generated by the Rodrigues formula

$$H_n(x) = (-1)^n e^{x^2} \frac{d^n}{dx^n}(e^{-x^2}).$$

Hermite functions are defined as[3, 4]

$$h_n(x) = \frac{1}{2^{n/2}\sqrt{n!}\sqrt{\pi}} H_n(x) e^{-\frac{x^2}{2}}. \quad (1)$$

This definition satisfies the orthonormality condition $\int_{-\infty}^{\infty} h_m(x)h_n(x)dx = \delta_{mn}$. The 2D band-limited Hermite expansion can be defined as[5]

$$f(\mathbf{x}) = f(x, y) = \sum_{m=0}^{N} \sum_{n=0}^{N-m} \check{f}_{mn} h_m(x)h_n(y), \quad (2)$$

where $\check{f}_{mn}$ is the Hermite coefficients.

Associated Laguerre polynomials are given by the Rodrigues formula,

$$L_n^k(x) = \frac{e^x x^{-k}}{n!} \frac{d^n}{dx^n}(e^{-x} x^{n+k}).$$

They are orthogonal over $[0, \infty)$ with respect to the weighting function $x^k e^{-x}$,

$$\int_0^{\infty} x^k e^{-x} L_m^k(x) L_n^k(x) dx = \frac{(n+k)!}{n!} \delta_{m,n}.$$

The band-limited Laguerre-Fourier expansion is defined as[5]

$$f(r, \theta) = \sum_{m=0}^{N} \sum_{n=-m}^{m} \tilde{f}_{mn} \chi_{mn}^*(r, \theta), \quad (3)$$

where c^* is the conjugate of c, $\tilde{f}_{mn}$ is the Laguerre-Fourier coefficients, $\chi_{m,n}(\rho, \theta)$ is defined as

$$\chi_{m,n}(\rho,\theta)=(-1)^{(m-|n|)/2}\sqrt{\frac{[(m-|n|)/2]!}{\pi[(m+|n|)/2]!}}\rho^{|n|}L_{(m-|n|)/2}^{|n|}(\rho^2)e^{-\rho^2/2}e^{-in\theta},$$

and $L_m^n(x)$ is the associated Laguerre polynomials.

In recent work,5 we have shown that the two band-limited expansions, (2) and (3), are equivalent to each other under the simple coordinate change, $x = r\cos\theta$ and $y = r\sin\theta$. Furthermore, the coefficients, $\hat{f}_{mn}$ and $\tilde{f}_{mn}$ are linearly related. The direct interconversion of the coefficients can be implemented as6

$$\widehat{f}_{k,m-k}=\sum_{n=-m}^{m}\tilde{f}_{m,n}Q_{k,n}^m\quad\text{and}\quad\tilde{f}_{m,n}=\sum_{k=0}^{m}\widehat{f}_{k,m-k}(Q_{k,n}^m)^*.$$

$Q_{k,n}^m$ is defined as

$$Q_{k,n}^m=\int_0^{2\pi}\int_0^\infty\chi_{m,n}^*(r,\theta)h_k(r\cos\theta)h_{m-k}(r\sin\theta)rdrd\theta,$$

and can be computed using the recurrence formula as

$$\begin{pmatrix}Q_{k+1,n+1}^{m+1}\\Q_{k,n+1}^{m+1}\end{pmatrix}=\frac{1}{2\sqrt{2}}\begin{pmatrix}\frac{1}{\sqrt{k+1}}&\frac{1}{\sqrt{k+1}}\\-\frac{i}{\sqrt{m-k+1}}&\frac{i}{\sqrt{m-k+1}}\end{pmatrix}\begin{pmatrix}\sqrt{m-n}Q_{k,n+2}^m\\\sqrt{m+n+2}Q_{k,n}^m\end{pmatrix},$$

and

$$\begin{pmatrix}Q_{k,n+1}^{m+1}\\Q_{k,n-1}^{m+1}\end{pmatrix}=\begin{pmatrix}\frac{1}{\sqrt{m+n+2}}&\frac{1}{\sqrt{m+n+2}}\\-\frac{1}{\sqrt{m-n+2}}&\frac{1}{\sqrt{m-n+2}}\end{pmatrix}\begin{pmatrix}i\sqrt{(m-k+1)}Q_{k,n}^m\\\sqrt{k}Q_{k-1,n}^m\end{pmatrix}.$$

2.2. Two-dimensional Band-limited Hermite Expansion Combined with Fourier Slice Theorem

Using a band-limited Hermite expansion with a large band limit, N, a 2D density can be approximated as (2) The rotated version of (2) is6

$$f(R^T\mathbf{x})=\sum_{m=0}^{N}\sum_{n=0}^{N-m}\check{f}_{mn}^\theta h_m(x)h_n(y)\quad(4)$$

where R is a 2×2 rotation matrix and θ is the angle of the rotation. The Hermite coefficients, $\check{f}_{mn}$ and $\check{f}_{mn}^\theta$ in (2) and (4) are linearly related to each other and the detailed relationship was derived in the previous work.6

The projection of (2) with the projection angle, θ, is equivalent to the projection of (4) along y axis, and it is written as

$$p_\theta(x)=\int_{-\infty}^{\infty}f(R^T\mathbf{x})dy=\sum_{m=0}^{N}\sum_{n=0}^{N-m}\check{f}_{mn}^{\theta}h_m(x)\int_{-\infty}^{\infty}h_n(y)dy=\sum_{m=0}^{N}\left(\sum_{n=0}^{N-m}\check{f}_{mn}^{\theta}s_n\right)h_m(x), \quad (5)$$

where $s_n = \int h_n(x)dx$. The value of s_n is zero when n is an odd number. $s_n=\frac{\sqrt{n!}\sqrt{\pi}}{\sqrt{2^{n-1}}(n/2)!}$, when n is even.[6] Note that this projection is also a one-dimensional band-limited Hermite expansion with the band limit, N. The Fourier transform of (5) is

$$\hat{p}_\theta(\omega)=\sum_{m=0}^{N}\left(\sum_{n=0}^{N-m}\check{f}_{mn}^{\theta}s_n\right)\sqrt{2\pi}(-i)^m h_m(\omega). \quad (6)$$

We used the fact that the Hermite functions are the eigenfunctions of the Fourier transform as[3]

$$\int_{-\infty}^{\infty}e^{-i\omega x}h_n(x)dx=\sqrt{2\pi}(-i)^n h_n(\omega). \quad (7)$$

The inverse Fourier transform of the Hermite functions can be derived as

$$\frac{1}{2\pi}\int_{-\infty}^{\infty}e^{i\omega x}h_n(\omega)d\omega=\frac{1}{\sqrt{2\pi}}(-i)^n h_n(-x)=\frac{1}{\sqrt{2\pi}}i^n h_n(x).$$

On the other hand, the two-dimensional Fourier transform of (2) is written as

$$\hat{f}(\omega_1,\omega_2)=\sum_{m=0}^{N}\sum_{n=0}^{N-m}\check{f}_{mn}(2\pi)(-i)^{m+n}h_m(\omega_1)h_n(\omega_2) \quad (8)$$

using (7).

Equation (6) is defined on the domain, $0 \le \theta < \pi$ and $-\infty < \omega < \infty$. The domain of (6) can be simply changed to $0 \le \theta < 2\pi$ and $0 \le \omega < \infty$ using the fact that $p_{\theta+\pi}(x) = p_\theta(-x)$ and $\hat{p}_{\theta+\pi}(\omega) = \hat{p}_\theta(-\omega)$. The Fourier slice theorem means that the two expressions, (6) and (8) are equivalent with the relation $\omega_1 = \omega\cos\theta$ and $\omega_2 = \omega\sin\theta$.

Since (8) is a band-limited Hermite expansion, its equivalent polar coordinate version can be express as a band-limited Laguerre-Fourier expansion as[5]

$$\hat{f}(\omega,\theta)=\sum_{m=0}^{N}\sum_{n=-m}^{m}\tilde{f}_{mn}\chi_{mn}^{*}(\omega,\theta). \quad (9)$$

It is important to notice that this coordinate conversion is lossless.

Therefore, (6), (8) and (9) are the equivalent expressions. Our goal is to obtain (8) from the projections using this equivalence and then perform the inverse Fourier transform to obtain the 2D original image.

2.3. Reconstruction Process

For each projection, $p_\theta(x)$, we obtain the corresponding Hermite expansion such that

$$p_\theta(x) = \sum_{m=0}^{N} \check{f}_m h_m(x)$$

Since the projection is given as a discrete data, we define a cost function to have the optimal coefficients as

$$C = \sum_{k=1}^{M} \left| p_\theta(x^{(k)}) - \sum_{m=0}^{N} \check{f}_m h_m(x^{(k)}) \right|^2,$$

where M is the number of samples of each projection. The optimal coefficients are given as the least-squared solution.[5]

The Fourier transform of the projection is given as

$$\widehat{p}_\theta(\omega) = \sum_{m=0}^{N} \check{f}_m \sqrt{2\pi}(-i)^m h_m(\omega)$$

Now we sample this function on a equally-spaced grid, (ω, θ). It is important to note that the sampled values are complex numbers. Since the coordinate conversion technique using Hermite and Laguerre-Fourier expansions was developed for the real-valued function, we need to separate the real part and the imaginary part of the sample values. Using the samples on a polar grid, we can have the Laguerre-Fourier expansions as

$$\widehat{f}(\omega, \theta) = \sum_{m=0}^{N} \sum_{n=-m}^{m} \tilde{f}_{mn}^r \chi_{mn}^*(\omega, \theta) + i \sum_{m=0}^{N} \sum_{n=-m}^{m} \tilde{f}_{mn}^i \chi_{mn}^*(\omega, \theta). \quad (10)$$

From the sample points, we can compute this Laguerre-Fourier expansion without loss of information. This is obvious because we have shown that (6) and (8) are equivalent using the Fourier slice theorem. The method to compute the Laguerre-Fourier coefficients from the samples on a polar grid is similar to the method to compute the Hermite coefficients from discrete data. The detailed method was proposed in the previous work.[5]

If we apply the coordinate conversion algorithm to (10), then we have

$$\widehat{f}(\omega_x, \omega_y) = \sum_{m=0}^{N} \sum_{n=0}^{N-m} \check{f}_{mn}^r h_m(\omega_x) h_n(\omega_y) + i \sum_{m=0}^{N} \sum_{n=0}^{N-m} \check{f}_{mn}^i h_m(\omega_x) h_n(\omega_y). \quad (11)$$

The inverse Fourier transform of (11) is

$$f(x,y) = \frac{1}{2\pi} \sum_{m=0}^{N} \sum_{n=0}^{N-m} (\breve{f}_{mn}^{r} + i\breve{f}_{mn}^{i})i^{m+n}h_m(x)h_n(y). \quad (12)$$

3. RESULTS

For simulation, we used two test images: the Shepp-Logan phantom (Fig. 2(a)) and a blob cartoon image (Fig. 3(a)). We computed the projections from 301×301 original images using 100 equally spaced projection angles in [0 π). We reconstructed the images from the projections using the Hermite-expansion-based method and the filtered backprojection method.

The reconstruction results by the new method are given in Fig. 2(b) and Fig. 3(b). We used the band limit $N = 240$. The absolute difference images between the original image and the reconstructed image are presented in Fig. 2(c) and Fig. 3(c). The absolute difference image, $d(x, y)$ between two images, $a(x, y)$ and $b(x, y)$ is defined as $d(x, y) = |a(x, y) - b(x, y)|$. In order to compare the new method to the classical filtered backprojection method, the reconstruction results by the filtered backprojection method are shown in Fig. 2(d) and Fig. 3(d). The corresponding difference images are shown Fig. 2(e) and Fig. 3(e).

The normalized least-squared errors (NLSE) between the original and the reconstructed images are shown in Table 1. In order to see the effect of the reconstruction methods on the meaningful part of the images, we clip the images using a window enclosing the meaningful area of the images. The new method shows the lower error in the blob image, while the filtered backprojection method is better with the Shepp-Logan phantom.

4. CONCLUSION

In this work, we showed how a band-limited Hermite expansion behaves under the parallel projection and reconstruction. Its special properties enable us to apply the Fourier slice theorem to the computed tomography problem directly without introducing an inexact interpolation for coordinate conversion or a non-integrable filter. In numerical simulations, we showed that the approach could solve the tomography problem.

Acknowledgments

References

1. Pan S, Kak A. A computational study of reconstruction algorithms for diffraction tomography: Interpolation versus filtered-backpropagation. IEEE Transactions on Acoustics, Speech, and Signal Processing. 1983; 31(5):1262–1275.

2. Miao J, Frster F, Levi O. Equally sloped tomography with oversampling reconstruction. Physical Review B. 2005; 72

3. Chirikjian, GS.; Kyatkin, AB. Engineering Applications of Noncommutative Harmonic Analysis. CRC Press; 2000.

4. Vilenkin, N.; Klimyk, A. Representation of Lie Groups and Special Functions. Kluwer Academic Publ; Dordrecht, Holland: 1991.

5. Park W, Chirikjian GS. Interconversion between truncated Cartesian and polar expansions of images. IEEE Transactions on Image Processing. 2007; 16(8):1946–1955. [PubMed: 17688200]

6. Park, W. PhD thesis. Johns Hopkins University; 2008. Inverse Problems in Structural Biology and Flexible Needle Steering.
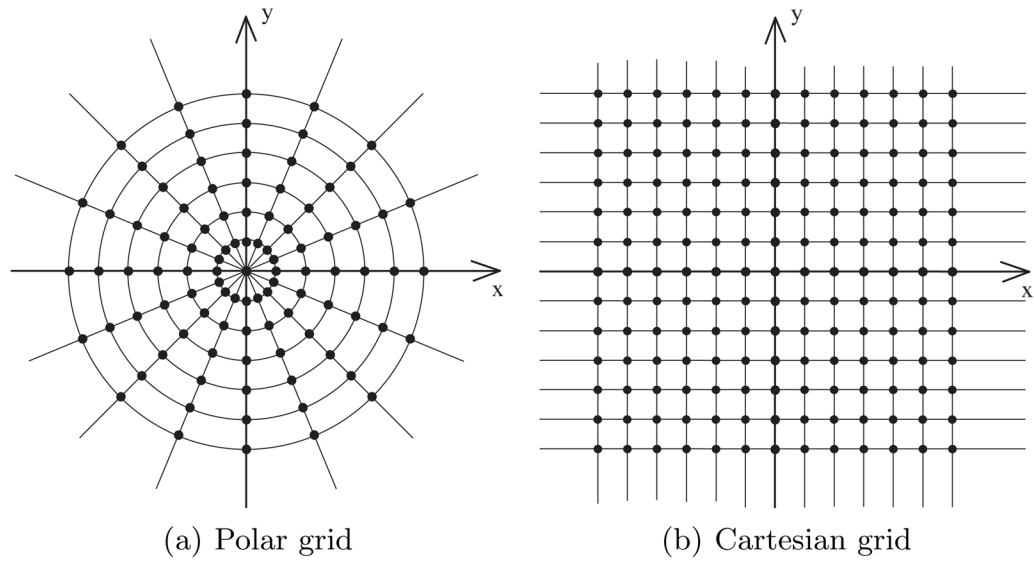
Figure 1.
Equally spaced grids

(a) Shepp-Logan image (301 × 301 pixels)
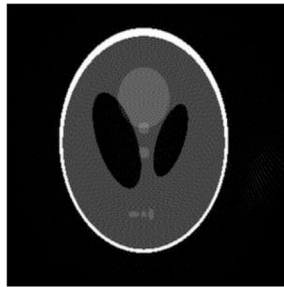
(b) Reconstructed image using Hermite expansions
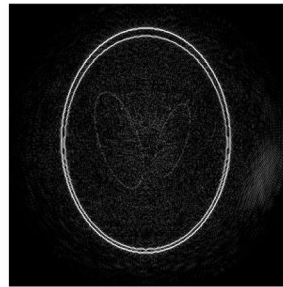
(c) Amplified (×3) difference image between Fig. 2(a) and Fig. 2(b)

(d) Reconstructed image using filtered backprojection
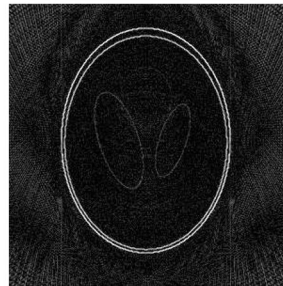
(e) Amplified (×3) difference image between Fig. 2(a) and Fig. 2(d)

Figure 2.
Tomography using Shepp-Logan phantom
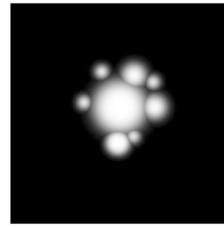
(a) Blob image (301 × 301 pixels)
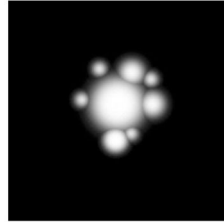
(b) Reconstructed image using Hermite expansions
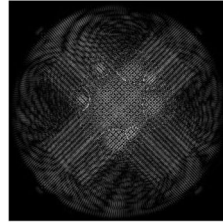
(c) Amplified (×50) difference image between Fig. 3(a) and Fig. 3(b)
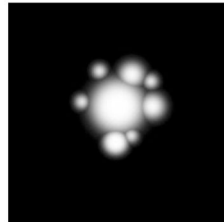
(d) Reconstructed image using filtered backprojection
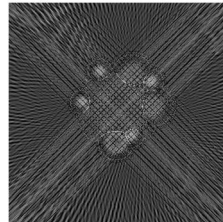
(e) Amplified (×50) difference image between Fig. 3(a) and Fig. 3(d)

Figure 3.
Blob cartoon test image

Table 1

NLSE in the reconstruction of Shepp-Logan phantom and the blob image.

	Shepp-Logan phantom	Blob image
Reconstruction using Hermite expansions	19.34%	1.14%
Filtered backprojection method	18.29%	1.45%